

SLAPSHOT: AN EFFICIENT MULTI-BAND MONTE CARLO SIMULATOR FOR SILICON

Xiao-Lin Wang, T. James Bordelon, Christine M. Maziar, and Al F. Tasch, Jr.

Microelectronics Research Center, The University of Texas at Austin, Austin, TX. 78712

Abstract

A new multi-band Monte Carlo model SLAPSHOT (SimuLation Program Suitable for HOt carrier sTudies), which combines high CPU efficiency and physical accuracy is described. This model uses an electronic bandstructure calculated by the pseudopotential method to generate a three dimensional scattering rate table and uses a fitted multi-valley, multi-band band model for electron free-flight and post-scattering momentum selection. The fitted bands include 65 valleys and their parameters are determined by fitting both the density of states and the $E(k)$ dispersion relation of the pseudopotential bands.

I. Introduction

The pressing need for accurately modeling high energy and nonlocal effects in deep submicron silicon MOSFETs makes Monte Carlo (MC) particle simulators a necessary tool for device engineers. One critical ingredient in all MC simulators is the electronic band structure of the material. The widely used simple parabolic or nonparabolic band model is not sufficiently accurate for modern deep-submicron devices in which high energy carriers complicate the device analysis. In order to model high energy processes accurately, Tang and Hess of Illinois[1] pioneered the use of the full band structure in their MC code. The “state of the art” of full band MC was further developed by Fischetti and Laux at IBM in their DAMOCLES code [2-3] which not only uses the full band $E(k)$ dispersion relation in the free flight, but also in electron-phonon dynamics (i.e. scattering rate calculations and momentum selection after scattering). This model, however, requires a tremendous amount of CPU resources and is costly for day-to-day device design. In order to improve computational efficiency, several authors have proposed new fitted band models[4-5]. In these approaches, the density of states (DOS) calculated from a full band is fitted with many isotropic nonparabolic bands. This approach introduces a tremendous savings in CPU time and partially includes the full band effect in the model. However, the $E(k)$ dispersion relation used in these models differs from that of the full band and may pose some problems. Even if the total scattering rate is accurately calculated, different $E(k)$ dispersion relations will bring carriers to different energy states during free flights and these states are coupled back to dynamical scattering and may well alter the scattering rate due to a wrong post free-flight electron energy. The incorrect dispersion relation also affects the calculation of electron velocity and position. This is serious because in modern devices the electric field may change very rapidly in space. Even a small error in electron position may result in putting the electron in a very different electric field. Moreover, using a fitted isotropic $E(k)$ relation also omits the anisotropy of the DOS during post-scattering momentum selection, which will lead to a similar problem.

II. Monte Carlo Model

In this paper, we describe a new model which uses both full band and fitted anisotropic multi-valley bands to address the above problems without a significant increase in the CPU time. In our model, phonon and ionized impurity scattering rates are calculated by using the first two pseudopotential energy bands. The numerical method used is the modified Gilat-Raubenheimer (G-R) approach [6-7] in where the Brillouin zone (BZ) is divided into small cubes and the argument inside of the energy conservation delta function is linearized (similar to the approach used in the IBM model[2]). The electron-phonon scattering rate is given by:

$$P_{\eta,\nu}(\vec{k}) = \sum_{\nu'} \frac{1}{(2\pi)^3} \int_{BZ} \frac{\pi}{\rho\omega_{\eta}(\vec{q})} \Delta_{\nu,\nu'}(\vec{q})^2 |g|^2 \delta(E_{\nu}(\vec{k}) - E_{\nu'}(\vec{k}') \mp \hbar\omega_{\eta}(\vec{q})) \binom{N_q + 1}{N_q} d^3k' \quad (1)$$

where η is a phonon mode, ν and ν' are initial and final band indices, Δ is a coupling constant, $|g|$ is the overlap integral (assumed to be unity in this paper). The phonon energy and occupation number is expressed as $\hbar\omega_{\eta}$ and N_q , respectively. A constant of 62 meV is used for the optical phonon and IBM's

acoustic phonon dispersion [2] is used for both longitudinal and transverse acoustic phonons. Equation (1) can only be evaluated accurately by the modified G-R method because of the complexity of the band structure and phonon dispersion relation. Both acoustic and optical phonon scattering rates can be written as summation of terms of the following form:

$$P(\vec{k}) = \int_{BZ} f(\vec{k}, \vec{q}) \delta(E_\nu(\vec{k}) - E_{\nu'}(\vec{k} \mp \vec{q}) \mp h\omega(\vec{q})) d^3q \quad (2)$$

The entire BZ is divided into tiny cubes and in each cube the argument inside of the delta function can be approximated by its first order Taylor series expansion:

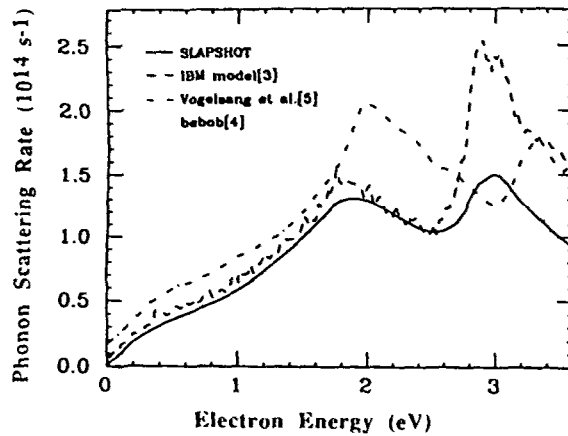
$$E_\nu(\vec{k}) - E_{\nu'}(\vec{k} \mp \vec{q}) \mp h\omega(\vec{q}) = A(\vec{k}, \vec{q}_m) + \vec{B}(\vec{k}, \vec{q}_m) \cdot \vec{q}' \quad (3)$$

Where \vec{q}_m is the center of the cube and \vec{q}' is the local phonon momentum as measured from the center of the cube. The volume element of the integration in each cube is separated as the product of the momentum projected on \vec{B} and the area perpendicular to \vec{B} inside of the cube $d^3q' = dq'S$. The three dimensional integration of scattering rate can then be written as the sum over all the cubes in the BZ.

$$P(\vec{k}) = \sum_{\vec{q}_m \in BZ} f(\vec{k}, \vec{q}_m) \frac{1}{|\vec{B}|} S_{\vec{B}}\left(-\frac{A}{|\vec{B}|}\right) \quad (4)$$

Where $A = E_\nu(\vec{k}) - E_{\nu'}(\vec{k} \mp \vec{q}_m) \mp h\omega(\vec{q}_m)$ and $\vec{B} = -\nabla E_{\nu'}(\vec{k} \mp \vec{q}_m) \mp h\nabla\omega_{\vec{q}}(\vec{q}_m)$. The area inside the cube on the plane $\vec{B} \cdot \vec{q}' + A = 0$ is given by $S_{\vec{B}}(|\vec{q}'|)$. The area S is then classified according to its distance A and orientation \vec{B} relative to the center of the cube. The formulae for each shape of S are given in reference [6-7]. Note that only when the gradient of phonon energy is zero is the scattering rate proportional to the density of states. This is another reason that the band structure model needs to fit both the DOS and the E(k) dispersion relationship. In this way, we are able to include the DOS effect as well as the complex anisotropy of the E(k) dispersion relation. This is especially important for silicon since the first band minima is very close to to the BZ edge and the second band minima and the existence of the zone edge decreases the DOS and makes the equi-energy surfaces distorted from the regular ellipsoidal shape. Although such calculations require a fair amount of CPU time, they only need to be done *once*. Figure 1 shows the total phonon scattering rate after the DOS weighted average. The slight difference from that of IBM[3] may be caused by our assumption of an unity overlap integral and slight different coupling constants.

Figure 1. Total electron-phonon scattering rate vs. electron energy calculated by averaging over the DOS of all valleys at 300K. IBM and other groups' scattering rates are also shown for comparison.



The scattering mechanisms included in this model are intravalley and intervalley acoustic phonon with both longitudinal and transverse modes, intravalley and intervalley optical phonon and ionized impurity scattering. The acoustic and optical phonon coupling constants are given below. We want to stress that only two coupling constants are used in our simulator for all electrons in the different valleys and different bands.

$$E_l - E_t = 1.8eV$$

$$DK = 3.4 \times 10^9 eV/cm$$

III. Fitted Multi-valley Band

For free flight and momentum selection after scattering, the fitted anisotropic multiple valley bands are used. The DOS of both pseudopotential bands and fitted bands are calculated by the G-R method described above. The effective masses and nonparabolicities of the 65 valleys of the fitted bands are determined by fitting the DOS (Fig. 2) and $E(k)$ dispersion relation (Fig. 3) of the first and second pseudopotential bands.

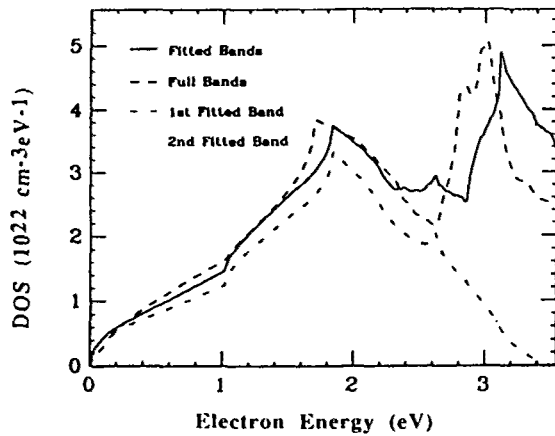


Figure 2. Comparison of DOS calculated from fitted bands and from pseudopotential bands.

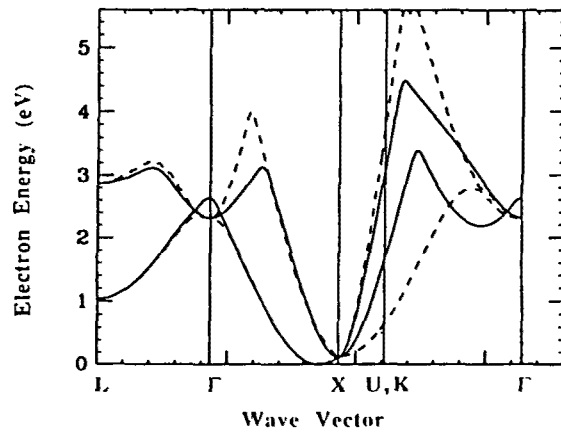


Figure 3. Comparison of $E(k)$ dispersion relation of fitted bands (solid line) and pseudopotential bands (dashed line) in several cuts along principal directions.

The boundaries of valleys are determined when two neighboring valleys have the same energy. The transitional regions are smoothed to provide a continuous electron energy and group velocity. The fitted bands satisfy all symmetries of the point group with correct degeneracy. The symmetry requirement restricts the number of effective masses to four in the first band and five in the second band. Table 1 lists the optimized band parameters for the first and second bands.

Table 1. The band parameters

Valley Index	Degeneracy	Orientation	$M_1 (m_0)$	$M_t (m_0)$	$\alpha (1/eV)$	$K_{min} (2\pi/a)$	$E_{min} (eV)$
00	6	{100}	0.87	0.31	0.20	0.85,0,0	0.0
01	24	{100}	0.87	0.31	0.20	1,1,0.15	0.0
02	8	{111}	1.60	0.22	0.065	0.5, .5, .5	1.04
10	6	{100}	0.30	0.12	0.28	1,0,0	0.13
11	12	{100}	0.30	0.12	0.28	1,1,0	0.13
12	1	{100}	0.55	0.55	0.80	0,0,0	2.31
13	8	{111}	2.70	0.65	0.20	0.5, .5, .5	2.87

Despite the fact that some valley minima fall outside of the BZ, part of the valleys are inside and those valleys are necessary to ensure the lattice translation symmetry and continuity of the band. The momentum selection after scattering is similar to IBM's "unified" model where all available states with correct final

energy are searched and one is chosen by a rejection method. The transitional probabilities of final valleys which are needed by the rejection method are precalculated just like the scattering rates. All scattering between the 65 valleys is included. The use of group theory greatly simplifies the complex algorithms of selecting the final band, valley and momentum, especially for acoustic phonon scattering where the scattering probability depends on both the DOS of the final valley and the phonon momentum. It also saves memory resources by storing the bandstructure and scattering rates only in the irreducible wedge which is only 1/48 of BZ. The CPU speed is also enhanced through the reduction of the search area of the bandstructure and scattering rate table. The symmetry operations (and their inverse) take very little CPU time since all point group operations are only a series of axis permutation and reflection and no 3 by 3 matrix manipulation is needed. Figures 4 and 5 display simulation results and compare them to available experimental data as well as results presented by other Monte Carlo researchers.

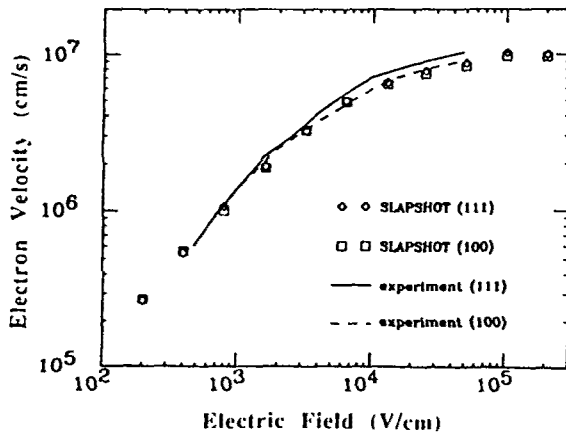


Figure 4. Electron drift velocity in (111) and (100) at 300K. Results are compared with experimental data from reference [9].

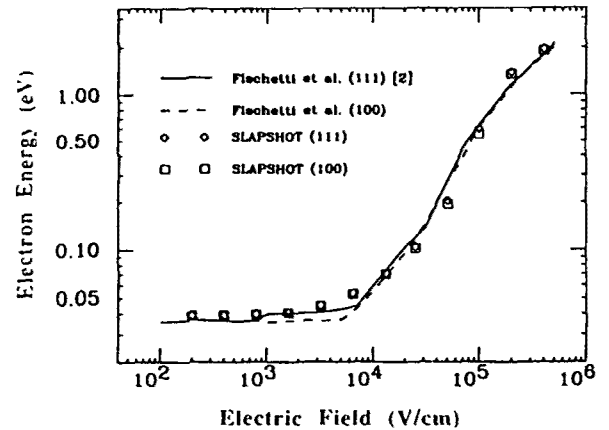


Figure 5. Simulated electron energy at room temperature for (111) and for (100). Data from reference [2] is also shown for comparison.

IV. Summary

In summary, we have developed a very highly efficient MC code which uses a full band structure for accurate scattering rate calculations and uses fitted bands for free flight and momentum selection after scattering. The anisotropic model band fits both the DOS and $E(k)$ dispersion in all principal directions. Using this model, we are able to get a high degree of accuracy in high energy transport with the efficiency of a simple single band simulation.

References

- [1] J. Y. Tang and K. Hess, *J. Appl. Phys.* **54**, 5139 (1983).
- [2] M. Fischetti, S. Laux, *Phys. Rev. B* **38**, 9721 (1988).
- [3] M. Fischetti, S. Laux, *IEEE Trans. Electron Devices* **ED-38**, 634 (1991).
- [4] R. Brunetti, C. Jacoboni, F. Venturi, E. Sangiorgi and B. Ricco, *Solid State Electron* **32**, 1663 (1989).
- [5] T. Vogelsang and W. Hänsch, *J. Appl. Phys.* **70**, 1493 (1991).
- [6] G. Gilat and L. J. Raubenheimer, *Phys. Rev.* **144**, 390 (1966).
- [7] G. Gilat and L. J. Raubenheimer, *Phys. Rev.* **147**, 670 (1966).
- [8] X. Wang and J. Bordelon, C. Maziar and A. Tasch, Jr. *Proc. International Semiconductor Device Research Symposium*, 239 (1991).
- [9] C. Canali, C. Jacobini, F. Nava, G. Ottaviani and A. Alberigi Quaranta, *Phys. Rev. B*, **12**, 2265 (1975).